Neuronal Damage in Murine Experimental Cerebral Malaria, Implications for Neuronal Repair and Sequelae

Monique F. Stins [1,2,3,*], Irene Gramaglia [2,†], Joyce Velez [2,†], Carlos A. Pardo [4] and Henri van der Heyde [2]

1   Malaria Research Institute, Johns Hopkins Bloomberg School of Public Health, Baltimore, MD 21205, USA
2   La Jolla Infectious Diseases Institute, LJIDI, San Diego, CA 92130, USA
3   Biomedical Research Institute of Southern California, Oceanside, CA 92046, USA
4   Department of Neurology, Division Neuroimmunology and Neurological Infections, Johns Hopkins School of Medicine, Baltimore, MD 21287, USA
*   Correspondence: mstins@jhmi.edu
†   Current address: Agilent Technologies, Santa Clara, CA 95051, USA.

Abstract: Cerebral malaria (CM) is a deadly complication of *P. falciparum* infection. Although adults with CM have a higher mortality rate, CM affects mostly children under the age of 5 years. Neurological symptoms and signs include impaired consciousness, coma, seizures, and increased intracranial hypertension. Upon survival of a CM episode, persistent neurologic deficits occur in a subset of surviving children. These sequelae include recurrent seizures, behavioral deficits, loss of developmental milestones, learning disabilities and attention deficit hyperactivity disorder, which can remain with the survivors. The underlying neuropathology of these post CM neurologic sequelae are unclear. Therefore, we probed the extensive neuronal damage that occurs in an experimental murine model of cerebral malaria (eCM), focusing on the hippocampus. In addition, we explored responses of neuro-progenitor cells (NPC's) and potential repair mechanisms. We report here that *Plasmodium* infection causes extensive neuronal damage in the hippocampus, characterized by a loss of neuronal NeuN and double cortin (DCX) immunostaining in eCM mice. On day 6 of eCM we also observed increased neurofilament light chain staining, indicative of neuronal fragmentation, which was accompanied by an increase in neurofilament light chain in CSF but not seen in plasma. A concomitant increase in the influx of neuroprogenitor cells in eCM was observed, suggesting ongoing neuronal repair.

Keywords: cerebral malaria; neurons; murine experimental malaria; blood brain barrier; NeuN; neurofilament light chain; DCX; myelin basic protein; neuroprogenitors

1. Introduction

CM is one of the serious complications of *P. falciparum* infection. Although adults with CM have a higher mortality rate, CM affects mainly children under the age of five [1,2]. Children who survive CM often remain with neurologic sequela that can be transient and disappear within 3 to 6 months or can persist for years [3]. Sadly, up to 30% of the children who survive CM have increased risks of life-long post-CM neurologic sequelae, including cognitive and behavioral problems [3–11]. In particular, neurological deficits can affect developmental milestones, cause attention deficit hyperactivity disorder and reduce quality of life and opportunities [9,12–16]. However, how the *Plasmodium* parasite causes these neurological symptoms is not fully understood.

The hallmark of CM is the sequestration of *Plasmodium*-infected red blood cells in the brain's vasculature. Interestingly, the intra-erythrocytic *Plasmodium* parasite does not

enter the brain by crossing the blood brain barrier (BBB) but still causes brain damage [17]. Several hypotheses have been outlined to explain the neuropathogenesis of CM, such as the mechanical hypothesis, based on the sequestrations of parasitized red blood cells, resulting in hypoperfusion and localized hypoxia [18,19]. Pimonidazole injections identified hypoxia in perivascular neurons, which was confirmed by increased immunoreactivity for hypoxia inducible factor-1 [20]. The hypoxia could contribute to neuronal damage near parasitized micro vessels, as shown in retinal examinations of CM patients [21]. BBB disruption is observed in CM [17,22,23] and neuroimaging in both human CM and in an experimental murine model for CM (eCM) shows evidence of cerebral edema [24–26]. The cytokine storm hypothesis [27], postulates that increased peripheral inflammation and circulating chemokines and cytokines significantly contributes to development of CM. Indeed, in addition to peripheral inflammation, high levels of neuroinflammation, as evidenced by the levels of chemokines and cytokines in the cerebrospinal fluid (CSF) [28–33], have been suggested to play a key role in CM neuropathogenesis [34]. With a key role for inflammation playing a role in both humans and murine eCM models, the resulting brain swelling can lead ultimately to the loss of life [21,24,25,35]. However, none of these single hypotheses are conclusive and explain the full course of neuronal damage underlying these neurological sequelae and additional host and parasite factors play a role. As we are interested in investigating the pathogenesis of neurological sequelea, we studied characteristics of the neurological damage that may contribute to the neurocognitive deficits in post-CM sequelae, focusing on the hippocampal formation.

The hippocampus, located in the medial temporal lobe, is involved in memory and cognitive function [36,37]. Regions of the hippocampus such as the dentate gyrus (DG) and cornu ammonis (CA) regions, which are central to the cognitive and memory networks, maintain a continuous replenishment of neurons. Hippocampal DG's newborn neurons are continuously added and develop into granule neurons that progressively extend their axons towards the CA2 and CA3 regions of the hippocampus [38]. Disruption of this process of neurogenesis can lead to seizure activity and cognitive dysfunction [39]. Neuro-inflammation may affect the brain during critical periods of brain development, pathological mechanisms that as occurs in CM, leading to alteration of newborn granule neurons, influencing survival, maturation and replacement of newborn neurons with subsequent long-term neuronal disturbances [40,41]. As memory and learning deficits have been observed in CM survivors, as well in murine experimental CM models [6,9,12–16,42,43], this study focuses on the hippocampal formation neuronal biology.

Neuropathological studies on human CM are limited due to the restricted availability of human CM brain samples. Studies with primate models of CM are very limited due to costs and ethical concerns. The development of experimental murine models of CM, which are low cost and availability of investigational tools, facilitate reliable assessment of the neurobiology of CM. The in vivo murine *Plasmodium berghei*-ANKA (PbA) experimental CM model replicates essential parts of human CM pathology, including the evidence of trapped parasitized red blood cells that disturb blood flow, vascular leakage, astro-neuronal damage, gliosis and impaired neurological dysfunction [42,44–48]. This makes the PbA eCM model a suitable and valuable tool to aid in the study of CM neuropathogenesis. Therefore, we used this widely used murine eCM model to study neuronal damage that may be responsible for the neurological sequelae in CM [42,44,45,47–49].

2. Materials and Methods

2.1. Chemicals and Reagents

Polyvinylpyrrolidone, sodium citrate, sodium tetraborate decahydrate, hydrochloric acid (HCl), ethylene glycol, 4′,6-diamidino-2-phynymindole (DAPI) nucleic acid stain,

Triton X-IOO, normal goat serum (NGS), and normal donkey serum (NDS) and a GIEMSA stain kit were purchased from Millipore-Sigma (Burlington, MA, USA). Sodium acetate was purchased from Fisher Scientific (Waltham, MA, USA). Heparin (cat#411210010) was from Acros Organics. The anti-proliferation marker Kiel67 (Ki-67) antibody (1:100) (cat# D3B5) and anti-neurofilament light chain (NFL) antibody (C28E10) (1:200) were purchased from Cell Signaling Technology (Danvers, MA, USA). Anti-bromodeoxyuridine (BrdU) antibody (1:1000) (cat # OOBT0030) was from BioRad/AbD Serotec (Hercules, CA, USA). Anti-doublecortin (DCX) antibody (1:250) (cat# sc-8066) was obtained from Santa Cruz Biotechnology (Dallas, TX, USA). Anti neuron-specific nuclear binding protein (NeuN) antibody (1:250) (cat# MAB3773) was from Millipore (Burlington, MA, USA). Anti-brain myelin protein (BMP) (cat # NB600-71755) antibody (1:200) was from Novus Biotechnologies. ELISA for neurofilament light chain (NFL) was purchased from MyBioSource (San Diego, CA, USA). Secondary antibodies: goat anti-rabbit Alexa fluor (AL) 488, donkey anti-mouse AL555, and donkey anti-goat AL633, donkey anti-mouse lgGIgG-AL555 antibody, goat anti-rat IgG-AL488 antibody, and goat anti-donkey IgG-AL633 were purchased from Life Technologies (Thermofisher, Carlsbad, CA, USA) and used at 1: 250. Prolong gold mounting media (Invitrogen cat#P36935). Phosphate Phosphate-buffered saline was purchased from Corning (Corning, NY, USA).

2.2. Animals

To induce experimental cerebral malaria (eCM), six to 10-week-old wild type C57 black mice (C57/Bl6) of both sexes were infected with *Plasmodium berghei* ANKA (PbA) (MR4-BEI resources, Manassas, VA, USA) at 10^6 PRBCs, intraperitoneal, as previously published [50,51]. The Institutional Animal Care and Use Committee (IACUC) of La Jolla Infectious Disease Institute approved all protocols and procedures. (#LJ14-01 3/7/2014). The mice were maintained on standard chow in standard ventilated cages with enrichment recommended and approved by IACUC. Four independent experiments with each 3–4 mice per group were done. In each experiment the development of disease was assessed daily by measuring the following clinical parameters: (1) righting and gripping reflexes (on a score of 0–5, with 5 exhibiting no impairment), (2) weight, (3) skin temperature, and (4) parasitemia, as previously published [52,53]. Parasitemia was assessed on thin blood films starting on day 4 and every 2 days after, until eCM or up to day 12 for mice that did not progress. Usually, 75–80% of mice would progress to full eCM by day 6. When eCM/neurological signs developed, mice were closely watched and euthanized before they became moribund (eCM score < 4). Only mice that had qualifying combined eCM scores included in this study. To follow neuroprogenitor cells, mice were injected with BrdU (10 mg/200 μL) 3 h before euthanasia, as described by Lee et al. [54]. Avertin (tribromoethanol) anesthetized mice were trans-cardially perfused by gravity with ~15 mL of phosphate buffered saline (PBS) containing 0.1 mg/mL heparin at 4 °C until clear fluid exited, followed by ~20 mL of freshly prepared 4% paraformaldehyde (PFA)/PBS at 4 °C. Whole brains were dissected and post-fixed in 20 mL 4% PFA overnight at 4 °C. Subsequently brains were cryoprotected in solutions with increasing sucrose concentration (15% to 30% sucrose/PBS) and kept at 4 °C. Brains were snap frozen in a clean 5 mL Eppendorf tube by immersion of the tube in 2-Methylbutane with dry ice and stored at −80 °C.

Blood was collected by retro-orbital bleed, as previously described [51], allowed to clot at RT for 30 min and centrifuged at 1500× *g* for 10 min in a refrigerated centrifuge at 4 °C. Serum was then aspirated and placed into fresh tube and frozen at −80 °C until analyzed. Cerebrospinal fluid (CSF) samples were obtained as a terminal procedure by cisternal puncture through the foramen magnum. A small hole was created in the membrane and using a pulled glass hematocrit capillary with a very fine point. CSF was withdrawn

through, as described [55]. Approximately 5–10 µL was obtained per mouse diluted in PBS and stored at −80 °C till analysis. Neurofilament light chain (NFL) was determined by ELISA in triplicate.

2.3. Preparation of Floating Brain Sections

Mouse brains that had been previously fixed with paraformaldehyde (PFA) and cryopreserved with sucrose were cut into ~40 µm sections using a sliding microtome (Microm HM440 E). Sections were collected in 48-well plates containing 500 µL section storage solution (1% polyvinylpyrrolidone, 40% ethylene glycol, 1M sodium acetate, at pH 6.5). Brain sections from the lateral ventricles and the hippocampus were used for immune-fluorescence incubations. Matching regions of interest for both control and PbA infected brains were selected with the microscope. Per condition, a minimum of 3 mice, with 3 to 4 sections per brain were evaluated. Prior to immunostaining, the sections were washed three times in PBS for 10 min and a fourth wash overnight. Sections probed for BrdU were pre-incubated in 1M HCl for 30 min at 37° C, followed by a 30-min incubation in borate buffer (0.1M sodium tetraborate decahydrate pH 8.5). Sections probed for the nuclear proliferation marker Ki-67 were pre-incubated in 10 mM sodium citrate, 0.05% Triton X-100, 6.0 pH that had been heated to 95 °C and allowed to cool at room temperature, together with the sections for a period of 45 min. All sections were then washed with PBS and blocked in blocking buffer (PBS 0.2% Triton X-100 with 5% normal donkey serum (NDS)), followed by an incubation with primary antibodies diluted in PBS-T 0.1% with 1% NDS. Sections were incubated at 4 °C with gentle rotational rocking for 48 h, washed three times with PBS and incubated in secondary antibodies diluted in PBS-T 0.1% with 1% NDS at 4 °C with gentle rocking for 24 h. During secondary antibody incubation, and in all subsequent steps, sections were shielded from light using aluminum foil to preserve fluorescence. Sections were then washed with PBS and incubated in 300 nM DAPI for 30 min followed by another wash in PBS and mounted onto slides with Prolong gold mounting media. The mounted slides were allowed to dry and viewed using a Zeiss Axioimager M2. Pictures of the sections were taken at same settings for all conditions and processed using Volocity image processing software, version 6.3 (Quorum Technologies). Alternatively, sections were scanned using a Panoramic P1000 scanner (courtesy of Rick Wolfe, Epredia) and viewed with Case viewer software. The background was subtracted with similar settings for all conditions and further cropped and assembled using Microsoft Power-Point.

2.4. Data Analysis

Immunofluorescence of brain sections was quantified using Image J/FIJI software (https://imagej.net/software/fiji/, accessed on 26 May 2025) [56]. A manual free shape was drawn around the area of interest (DG and CA regions) for each fluorescent channel and the integrated density was measured. The fluorescence intensity was normalized to the selected area to obtain the mean pixel density per area. Results were reported as percentage control to make comparisons between separate experiments. GraphPad Prism 6.0 software (GraphPad Software; San Diego, CA, USA) and MS Excell were used for statistical analysis. Standard statistical procedures were followed and unless otherwise stated, the data were expressed as mean ± standard error of the mean (SEM). Total Ki67(+) or BrdU + cell numbers were manually counted and analyzed for statistical significance by Student's *t*-test.

3. Results

3.1. Neuronal Damage and Altered Morphology in eCM

During the course of the PbA infection, parasitemia increased to $8.2 \pm 1.03\%$ on day 6. At that time the eCM signs were apparent with eCM clinical scores between 4 and 6 were included, similar to our previous publications [50–52,57]. At that time the mice were euthanized, brains dissected and compared with non-infected control mice. Changes in immunostaining for neurons, neuronal progenitors and myelin were assessed in floating sliding sections, as described in the material and methods section. Mature neurons were visualized with anti-NeuN immunostaining, and in the control non-infected mice this revealed the characteristic hippocampal architecture and clear NeuN immuno staining (Figure 1). PbA infection resulted in eCM and a decrease in anti-NeuN immune staining of the hippocampus, indicating a loss of neurons in both DG and CA hippocampal formations.
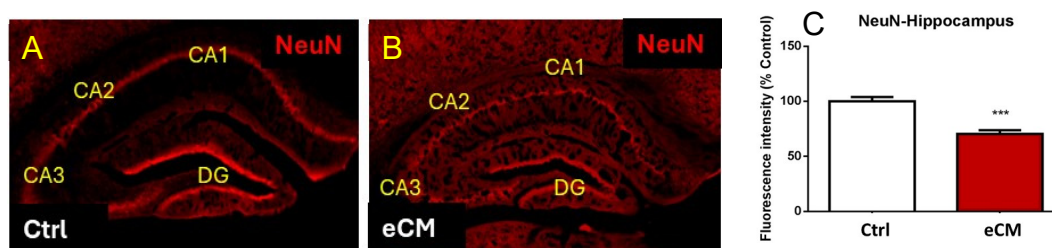

Figure 1. Neuronal damage in eCM. Mature neurons in hippocampus were labeled with anti NeuN-antibody in free floating sections of both control and PbA infected eCM brains. Sections were scanned and post magnification was 5X. (**A**) Control hippocampal neurons showed their characteristic hippocampal architectural pattern. (**B**) At the onset of eCM loss of neuronal anti-NeuN immune staining (red) was observed. (**C**) Quantification of a representative experiment (DG and CA areas) showing decreased NeuN staining over the time course of eCM. (Mean $\pm$ SEM graphed, Control n = 6, eCM n = 5, *** $p < 0.05$).

As we observed a loss in NeuN neuronal immunostaining, we tested if there would be additional axonal damage by immunolabeling for both myelin basic protein (MBP) and neurofilament light chain (NFL) (Figure 2). This showed an increase in NFL (red) immunostaining and decreased MBP (green) immune staining in eCM, suggesting increased neurofilament breakdown and loss of myelin in eCM brains compared to the control non-infected mice. Especially in the CA1, CA2 and DG areas of the hippocampus, a striking reduction in MBP staining was observed ($p < 0.05$) (Figure 2G–J). These neuronal changes in both NeuN and MBP staining did not appear to be specific to the hippocampus, as the cortical areas were also affected, revealing decreased and 'interrupted' MBP immunostaining in eCM.
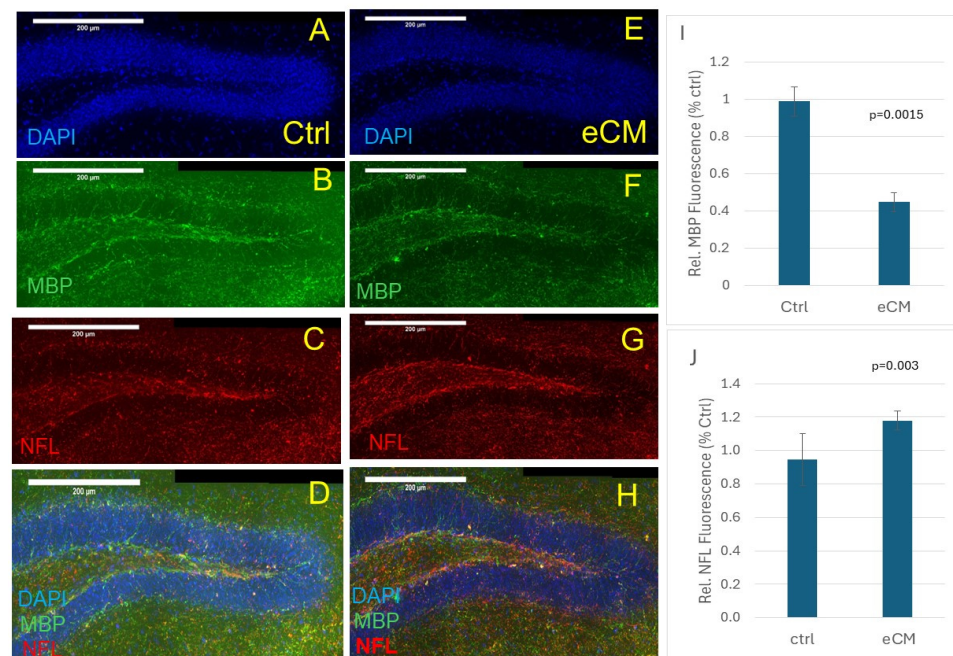
3.2. Increased NFL and Decreased MBP Immunostaining in the Hippocampus in eCM

Further focusing on the DG area of the hippocampus, anti-MBP immunostaining (green) was clearly present in the control non-infected mice (Figure 3B). Also here, immunostaining for MBP showed a significant loss of myelin in eCM brains compared to the controls (Figure 3F) ($p = 0.0015$), confirming the above findings. As we observed the loss of total anti-NeuN immune staining of the neurons, we also assessed the appearance of axonal breakdown products, such as fragments of the neurofilament light chain (NFL) (Figure 3). A clear increase in red NFL immunostaining was seen in the eCM sections (Figure 3G) ($p = 0.003$), especially in the DG area, confirming significant axonal damage.
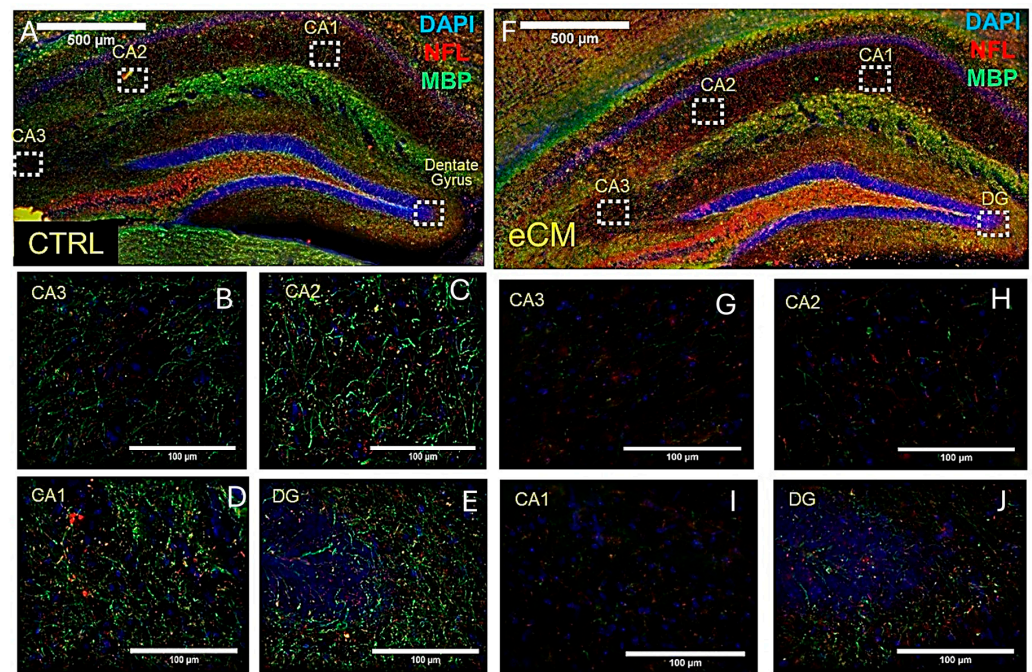
Figure 2. Visualization of neurofilament and myelin damage in eCM. Overview of immunolabeling for neurofilament light chain (NFL) and myelin basic protein (MBP), in a control non-infected mouse (Ctrl) at day 0 and at eCM (bar (**A**,**B**) = 500 μM and bar (**B–E**), (**G–J**) = 100 μM). (**A**): overview of Day 0 (left panel, (**A**)) shows MBP (green), NFL (red) staining and DAPI (blue). Right panel (**F**,**J**) shows a section from eCM mice. Compared with the control, MBP staining decreased and NFL staining increased in eCM. The bar is 500 microns. Bottom panels: higher magnification and details of indicated areas of the upper figures ((**B–E**) = control) and ((**G–J**) = eCM). The bar is 100 microns.

Figure 3. Neuronal damage in the hippocampal DG area. Showing increased NFL (red) immunostaining (**C**,**G**) as well as decreased MBP (green) (**B**,**F**) immunostaining at eCM (**E–H**) compared to control (**A–D**). Merged pictures shown in (**D**,**H**). Quantification of immunostaining in the DG center for MBP ((**I**), $p = 0.0015$) and NFL ((**J**), $p = 0.003$) for eCM compared to control (n = 3 per group). Mean ± SEM, Bar is 200 microns.

Concomitantly with the decline of NeuN immunostaining, the appearance of neurofilament light chain (NFL) fragments can be followed in cerebrospinal fluid (CSF) (Figure 4A). As determined by ELISA, about a 4-fold increase in the presence of NFL was observed in the CSF of the eCM mice on day 6 compared to the control mice ($p < 0.05$). The concentration of NFL in serum was much lower than in the CSF, and no significant difference in serum NFL concentrations were observed in eCM compared to non-infected control mice (Figure 4B).
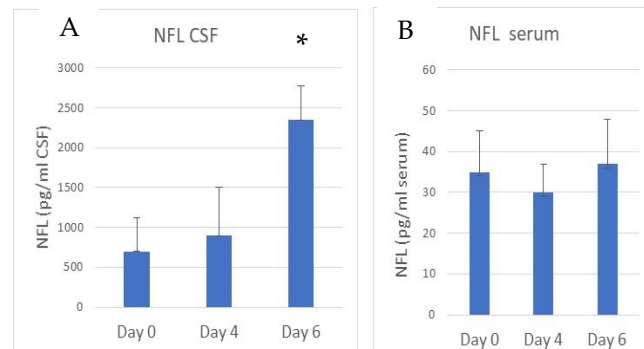

Figure 4. Quantification of appearance of neurofilament light chain in the CSF during eCM. (**A**) Time course of increased amount of neurofilament light chain (NFL) in CSF of PbA infected mice on day 4 and 6, compared to control non-infected mice at day 0. (n = 4 per group) (* $p < 0.05$ compared day 6 to day 0). (**B**) NFL concentration in serum of PbA infected mice on day 4 and 6 compared to day 0. Note the scale difference with high amount of NFL in CSF at day 6 but consistently low amounts of NFL in serum.

These results confirmed that neuronal damage occurs in eCM, as evidenced by the decrease in NeuN neuronal staining and the appearance of breakdown products in the form of NFL both in the brain tissue and in the CSF.

3.3. Decrease in Immature Neurons and Increased Neuroprogenitors in the Hippocampus During eCM

As neuronal immunostaining decreased during the course of eCM, we assessed whether neuronal repair would occur and if neuroprogenitor cells would migrate to areas of neuronal damage. Proliferating neuroprogenitor cells were identified both by BrdU incorporation or presence of the nuclear cell cycle regulating protein Ki67. Neuroprogenitors reside along the lining of the lateral ventricles [17]. In control mice, few BrdU- or Ki67-positive cells were present along the ventricles and in the DG of the hippocampus of control non-infected mice (Figure 5A). However, their numbers significantly increased with PbA infection and eCM development ($p = 0.02$) (Figure 6B). A large increase in their numbers was seen along the ventricle lining and in the DG areas in eCM (Figure 5G). This indicates that there is proliferation of neuroprogenitors and a resulting influx of NPCs into the hippocampus DG area, implicating that neuronal repair is attempted during eCM.

The numbers of immature neurons, as assessed by anti-DCX immune staining, decreased in eCM compared to controls (Figure 6), indicating that immature neurons in both the CA and DG areas of the hippocampus were affected in eCM. These results indicate that in PbA infected mice that develop eCM an increasing amount of neuronal damage occurs, involving both mature neurons, as shown above but also immature neurons.
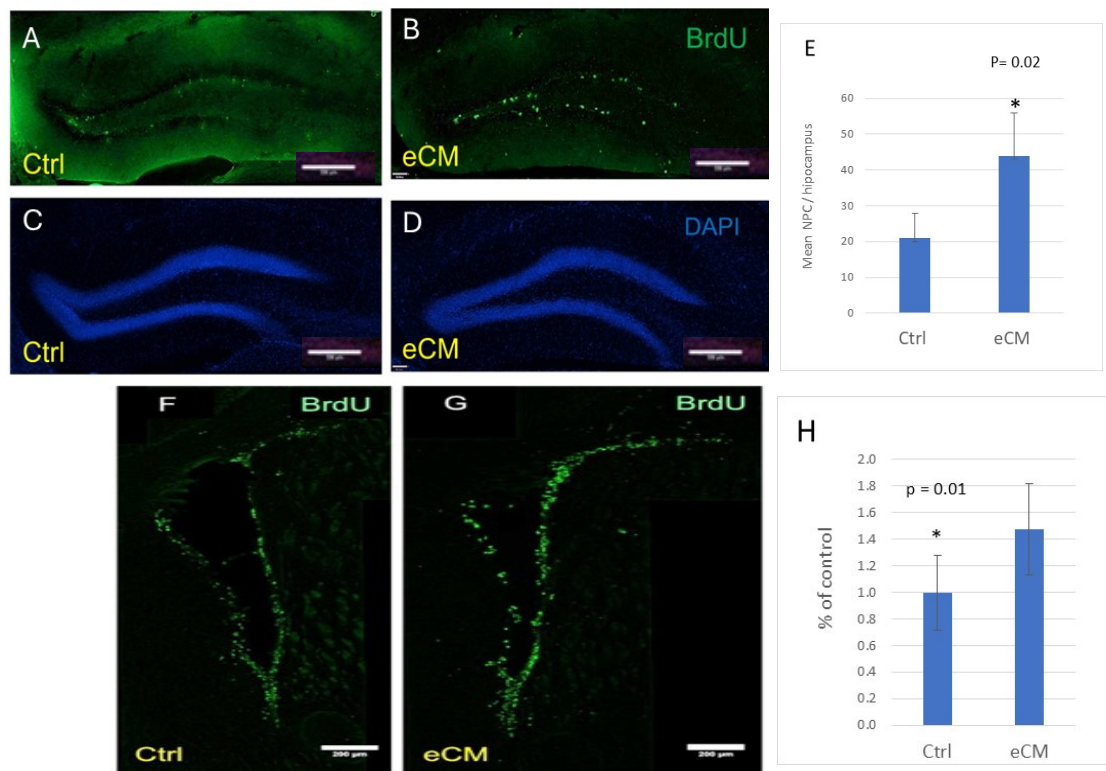
Figure 5. Increase in neuroprogenitors in eCM. Increased numbers of neuroprogenitors were observed in eCM. (**A,B**) Presence of proliferating progenitor cells were assessed by BrdU positive cells (green) in the dentate gyrus. (**C,D**) Nuclear DAPI staining (blue), (**E**) quantification of BrdU-positive progenitors in eCM shows an increase in BrdU+ cell numbers (* $p = 0.02$). (**F,G**) Increase in the number of BrdU+ neuroprogenitors and their staining intensity around the lateral ventricle in eCM compared to control noninfected mice (* $p = 0.01$). (**E,H**) Mean ± SD in eCM compared to Ctrl is shown. Bar = 200 μm.
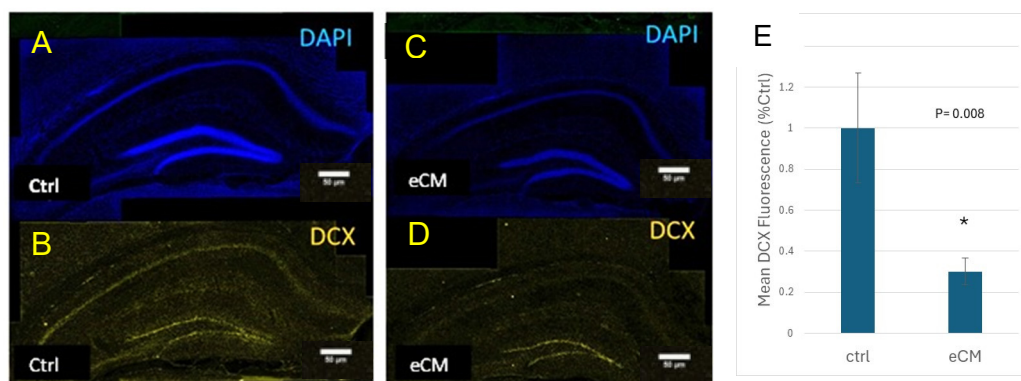
Figure 6. Decreased presence of immature DCX+ progenitors in eCM. To assess the fate of immature neurons during eCM, free floating sections of both control and the PbA infected eCM brains were labeled with anti DCX antibody. (**A,B**) Control hippocampus sections revealed DCX immune staining (yellow) in the hippocampus. (**C,D**) Sections of eCM brains showed loss of DCX staining in the DG area but a more pronounced loss of expression was observed in the CA areas. (**E**) Quantification shows decreased DCX staining in the DG area of control and eCM. Nuclear staining by DAPI is in blue DCX in yellow/orange. Mean + SEM is shown. (* $p = 0.008$) (n = 3 per group). Bar = 50 μm.

4. Discussion

Using an experimental murine model for CM to further characterize the underlying pathogenic processes we found that extensive neurological damage occurs during eCM, which is in agreement with others [47]. As we were interested in cognitive sequelae, we focused on the hippocampal formation, one of the areas involved in memory and

cognition. In the hippocampus, a loss of neurons and myelin was observed, as evidenced by the decreased NeuN- and MBP- immunostaining. Neuronal damage has also been documented in human CM [17,58]. Murine eCM neuropathogenesis also shows evidence of neuronal damage, including increased β-APP staining and tau [45,47]. In contrast, DeSousa et al. [46] did not report any glial-neuronal damage in PbA-infected mice as assessed by FluoJade and anti Iba-1 staining, although they found altered biochemistry and evidence of oxidative damage.

The loss of NeuN immunostaining in the mice in our study was accompanied by a significant increase in NFL fragments. NFL is a marker of axonal damage [59]. In the brains of eCM mice the NFL fragments were released into the CSF and values of up to ~2250 pg/mL, were observed, up from a baseline level of about 700 pg/mL NFL, as determined by ELISA. However, we did not observe a change in serum NFL concentrations in eCM compared to control mice, which was low (~35 pg/mL). Wai et. al. [60] reported neurofilament loss in axons and an increase in NFL plasma values of 317–528 pg/mL in eCM, depending on the level of edema compared to values of ~103 pg/mL in control mice. MRI imaging and electron microscopy of the olfactory bulb, cortex and brainstem also showed a loss of axonal structures, decrease in density and rearrangements of neurofilament in eCM. However, this group did not find a clear correlation of NFL levels with the outcome of the eCM, but did establish that some regeneration of the filaments in the axons occurred. Our immunofluorescent studies with NeuN in the hippocampus also showed a loss of axo-neuronal integrity and appearance of NFL fragments. Our values of NFL in eCM are higher than those of Wai et al. [60], but this can be due to the different methodologies used, such as, intra venous injection of sporozoites in the Wai study versus intra peritoneal injection of PbA infected red blood cells, as in this study. This shows that *Plasmodium* infection has an overall effect on the brain. The fact that we only saw an increase in NFL concentration in the CSF and not in the serum NFL values, could have several underlying causes. As intravenous injection of sporozoites [60] would involve the liver stage, this may lead to differences in timeline and severity of eCM between these two approaches. Like in human CM [21,25,35] there is also edema formation in eCM [24], therefore, there could be a differential dysfunction of the BBB and/or glymphatic drainage into the peripheral circulation. This may affect the appearance of peripherally circulating NFL in eCM, at this stage. However, to clarify this aspect additional future studies would be needed.

The observations on neuronal damage in eCM agree with previously published data on human CM [17,58]. There are limited studies on NFL in CSF and serum in CM, but recently, Balanza et.al [61] reported an in increase in NFL in plasma of African children with uncomplicated malaria and severe malaria. This group reported that NFL levels were higher in more severe cases and when the patients showed neurological manifestations. Datta et al. [62] 2023 also reported an increase in circulating NFL levels in pediatric patients with CM who died, but no CSF levels were reported. Interestingly, they found that elevated circulating NFL levels in patients were associated with worse attention and cognitive testing in children > 5 yrs [63].

In addition to the decrease in NFL, additional axonal damage was found as immunostaining for MBP was significantly decreased. This indicates a loss of myelin around the axons, affecting neuronal transmission. This was apparent in the hippocampal formation, where all areas (CA1-3 and DG) were affected. In addition, we found loss of immunostaining for MBP in other areas of the brain, such as the anterior Cingulate area and secondary motor areas. While assessing the effect on iron on the course and severity of eCM, Leitner et al. [64] also reported loss of MBP in mouse brain fractions. This group postulated that iron deficiency, either by diet or due to infection could lead to more severe myelin damage. Histological analysis in hematoxylin-eosin stain eCM brain sections showed myelin pal-

lor and fragmentation adjacent to congested capillaries [20]. Subsequent ultrastructural studies by this group showed a pathological changes and myelin abnormalities in the corpus callosum in eCM [65], suggesting vulnerability of the oligodendrocytes in eCM and possibly CM as well. Our studies showed a loss of myelin by MBP immune staining in the hippocampus and cortical brain areas. Due to the cellular organization in the hippocampus the neuronal damage, e.g., decreased NeuN and increased NFL immunostaining, appeared more striking in the hippocampal area than in the cortical areas. Neuronal damage in these areas could be similar, but on the other hand, given the inflammatory brain environment in eCM, it is possible that the hippocampal neurons are more sensitive to inflammation and changes in their environment than cortical neurons. In fact, Noel et al. [66] showed that hippocampal neurons were indeed more susceptible to caspases than striatal neurons [66]. Which is of relevance as caspases are also increased in CM [67]. In addition, as *Plasmodium* infection remains intravascular and the parasite does not cross the BBB, it is possible that vascular heterogeneity could play a role as well. Intravascular sequestration and circulating parasite and host factors may have a differential effect on different parts of the vasculature. Hippocampal microvessels may respond differentially in eCM than, for example, vessels in the corpus callosum or cortex. In addition, adjacent hippocampal neurons could be more sensitive to vascular inflammation than cortical neurons. Especially as we are recognizing more and more that vascular heterogeneity may play a role in diverse neurological diseases [68], hippocampal versus cortical brain areas may respond differently in eCM and/or other infections.

The underlying causes for this type of neuronal damage are unclear, but could involve the increased presence of metalloproteases, calpain and/or caspases, as shown in both eCM and CM [67,69]. In addition, the influx of immune cells, such as pathogenic CD8 T cells, which is observed both in murine CM and human CM, can contribute to this [49,70]. Moreover, interactions of PRBC's, circulating parasite factors and elevated coagulation factors with the endothelium of the BBB causes the brain vascular inflammation leading to a shift in release of chemokines and growth factors from the BBB into the brain, and thus directly or indirectly contributing to the observed neuronal damage [71–74].

Under normal healthy conditions, neuronal differentiation and growth occurs, especially in the young and growing brain. Neuroprogenitors present in the brain receive cues from their immediate environment to differentiate into the cellular type needed. There are at least two different types of progenitor cells present in the hippocampus: neuronal progenitor cells and oligodendrocyte progenitor cells (see Bonaguidi et al. for a review [75]). However, the identity, fate and functions of these different progenitor cells may overlap during pathological processes. In addition, these different types of progenitors may have a different sensitivity in inflammatory environments. Differential sensitivity of immature versus mature neurons to toxins has been shown in vitro [76]. It is thought that DCX+ progenitors contribute to the generation of oligodendrocytes [77]. The neuro-progenitors from the subventricular zones and DG are thought to differentiate into neurons [77,78].

In the eCM model we see that the immature DCX-positive neurons disappear, possibly because these cells are very sensitive to the highly inflammatory environment in the eCM brain. DCX-positive neurons are also disappearing in other neurological conditions, including multiple sclerosis and cognitive impairments. De Miranda [79] also reported a decrease in DCX positive cells in eCM, concomitant with an increase in inflammatory factors and decreased growth factors, such as brain derived neurotrophic factor and nerve growth factor. In eCM, this could result in the observed myelin damage and reduced MBP immunostaining. At the same time as the DCX+ neurons are disappearing, a large influx of the Ki67/BrdU + progenitors are seen. These cells are located along the lining of the ventricles, along the brain vasculature and in the hippocampus as well [80]. Although we

found evidence of neuronal damage in eCM, simultaneous aspects of neuronal repair are observed in eCM. The neuroprogenitors are activated by inflammatory environments, as is the case in the eCM brain [81]. Although the inflammatory eCM environment can trigger progenitor recruitment to sites of injury, expansion of the numbers and differentiation of the progenitors, excessive inflammation can also deregulate the differentiation process and neuronal renewal. Likely, these cells are recruited to the DG in order to repair the neuronal damage in eCM. Depending on whether these newly arrived progenitors receive the proper differentiation cues, there may be a full repair or recovery or with partial repair, cognitive neurologic sequelae may remain.

5. Conclusions

CM episodes can result in severe neurologic damage leading to cognitive and behavioral sequelae. In eCM we observed overall neurological damage, such as a loss of NeuN, BMP and increased NFL immune staining. We focused on the hippocampal formation, where we observed a profound decrease in neuronal staining and decreased myelin. In eCM, the brain responded with proliferation and recruitment of neuroprogenitor cells. Further research is needed into the mechanisms of hippocampal injury and repair in CM and the murine eCM model can be used as a reliable model for such studies. In CM patients, post CM-episode follow-up and testing indicated a spectrum of both short and long-term effects [6,82,83]. As certain sequelae are short term, mechanisms to repair the neuronal damage must be in place and the various neuroprogenitor cells can perform these functions. How these processes are exactly regulated and how to steer the neuronal repair process into the direction of full recovery is yet unclear and should be included in the focus of future research efforts. This may not only benefit CM patients but also those that recover from other brain infections and conditions.

Abbreviations

The following abbreviations are used in this manuscript:

eCM	experimental Cerebral Malaria
CSF	cerebrospinal fluid
DAPI	4′,6-diamidino-2-phenylindole
DCX	Double Cortin
DG	Dentate Gyrus
IACUC	Institutional Animal Care Committee
NFL	neurofilament fragments
PbA	*Plasmodium Berghei* ANKA
PBS	Phosphate buffered saline
PFA	paraformaldehyde
PRBC	*Plasmodium* infected red blood cells

References

1. Weiss, D.J.; Lucas, T.C.D.; Nguyen, M.; Nandi, A.K.; Bisanzio, D.; Battle, K.E.; Cameron, E.; Twohig, K.A.; Pfeffer, D.A.; Rozier, J.A.; et al. Mapping the global prevalence, incidence, and mortality of Plasmodium falciparum, 2000–2017: A spatial and temporal modelling study. *Lancet* **2019**, *394*, 322–331. [CrossRef] [PubMed] [PubMed Central]
2. World Health Organization. *World Malaria Report 2024: Addressing Inequity in the Global Malaria Response*; World Health Organization: Geneva, Switzerland, 2024; ISBN 978-92-4-010444-0.
3. Carter, J.A.; Mung'ala-Odera, V.; Neville, B.G.; Murira, G.; Mturi, N.; Musumba, C.; Newton, C.R. Persistent neurocognitive impairments associated with severe falciparum malaria in Kenyan children. *J. Neurol. Neurosurg. Psychiatry* **2005**, *76*, 476–481. [CrossRef] [PubMed] [PubMed Central]
4. Idro, R.; Carter, J.A.; Fegan, G.; Neville, B.G.; Newton, C.R. Risk factors for persisting neurological and cognitive impairments following cerebral malaria. *Arch. Dis. Child.* **2006**, *91*, 142–148. [CrossRef] [PubMed] [PubMed Central]
5. Idro, R.; Kakooza-Mwesige, A.; Balyejjussa, S.; Mirembe, G.; Mugasha, C.; Tugumisirize, J.; Byarugaba, J. Severe neurological sequelae and behaviour problems after cerebral malaria in Ugandan children. *BMC Res. Notes* **2010**, *3*, 104. [CrossRef] [PubMed] [PubMed Central]
6. John, C.C.; Panoskaltsis-Mortari, A.; Opoka, R.O.; Park, G.S.; Orchard, P.J.; Jurek, A.M.; Idro, R.; Byarugaba, J.; Boivin, M.J. Cerebrospinal fluid cytokine levels and cognitive impairment in cerebral malaria. *Am. J. Trop. Med. Hyg.* **2008**, *78*, 198–205. [CrossRef] [PubMed] [PubMed Central]
7. Langfitt, J.T.; McDermott, M.P.; Brim, R.; Mboma, S.; Potchen, M.J.; Kampondeni, S.D.; Seydel, K.B.; Semrud-Clikeman, M.; Taylor, T.E. Neurodevelopmental Impairments 1 Year After Cerebral Malaria. *Pediatrics* **2019**, *143*, e20181026. [CrossRef] [PubMed]
8. Kihara, M.; Carter, J.A.; Newton, C.R. The effect of Plasmodium falciparum on cognition: A systematic review. *Trop. Med. Int. Health* **2006**, *11*, 386–397. [CrossRef] [PubMed]
9. Birbeck, G.L.; Beare, N.; Lewallen, S.; Glover, S.J.; Molyneux, M.E.; Kaplan, P.W.; Taylor, T.E. Identification of malaria retinopathy improves the specificity of the clinical diagnosis of cerebral malaria: Findings from a prospective cohort study. *Am. J. Trop. Med. Hyg.* **2010**, *82*, 231–234. [CrossRef] [PubMed] [PubMed Central]
10. Kariuki, S.M.; Abubakar, A.; Newton, C.R.; Kihara, M. Impairment of executive function in Kenyan children exposed to severe falciparum malaria with neurological involvement. *Malar. J.* **2014**, *13*, 365. [CrossRef] [PubMed] [PubMed Central]
11. Carter, J.A.; Murira, G.M.; Ross, A.J.; Mung'ala-Odera, V.; Newton, C.R. Speech and language sequelae of severe malaria in Kenyan children. *Brain Inj.* **2003**, *17*, 217–224. [CrossRef] [PubMed]
12. Idro, R.; Marsh, K.; John, C.; Newton, C. Cerebral malaria: Mechanisms of brain injury and strategies for improved neurocognitive outcome. *Pediatr. Res.* **2010**, *68*, 267–274. [CrossRef] [PubMed]
13. Bangirana, P.; Menk, J.; John, C.C.; Boivin, M.J.; Hodges, J.S. The association between cognition and academic performance in Ugandan children surviving malaria with neurological involvement. *PLoS ONE* **2013**, *8*, e55653. [CrossRef] [PubMed] [PubMed Central]
14. Ruiseñor-Escudero, H.; Familiar, I.; Nyakato, M.; Kutessa, A.; Namukooli, J.; Ssesanga, T.; Joyce, C.; Laughton, B.; Grab, J.; Chernoff, M.; et al. Building capacity in neurodevelopment assessment of children in sub-Saharan Africa: A quality assurance model to implement standardized neurodevelopment testing. *Child. Neuropsychol.* **2019**, *25*, 466–481. [CrossRef] [PubMed] [PubMed Central]
15. Rosa-Gonçalves, P.; Ribeiro-Gomes, F.L.; Daniel-Ribeiro, C.T. Malaria Related Neurocognitive Deficits and Behavioral Alterations. *Front. Cell. Infect. Microbiol.* **2022**, *12*, 829413. [CrossRef] [PubMed] [PubMed Central]

16. Ssemata, A.S.; Nakitende, A.J.; Kizito, S.; Thomas, M.R.; Islam, S.; Bangirana, P.; Nakasujja, N.; Yang, Z.; Yu, Y.; Tran, T.M.; et al. Association of severe malaria with cognitive and behavioural outcomes in low- and middle-income countries: A meta-analysis and systematic review. *Malar. J.* **2023**, *22*, 227. [CrossRef] [PubMed] [PubMed Central]

17. Dorovini-Zis, K.; Schmidt, K.; Huynh, H.; Fu, W.; Whitten, R.O.; Milner, D.; Kamiza, S.; Molyneux, M.; Taylor, T.E. The neuropathology of fatal cerebral malaria in malawian children. *Am. J. Pathol.* **2011**, *178*, 2146–2158. [CrossRef] [PubMed] [PubMed Central]

18. White, N.J.; Warrell, D.A.; Looareesuwan, S.; Chanthavanich, P.; Phillips, R.E.; Pongpaew, P. Pathophysiological and prognostic significance of cerebrospinal-fluid lactate in cerebral malaria. *Lancet* **1985**, *1*, 776–778. [CrossRef] [PubMed]

19. MacPherson, G.G.; Warrell, M.J.; White, N.J.; Looareesuwan, S.; Warrell, D.A. Human cerebral malaria. A quantitative ultrastructural analysis of parasitized erythrocyte sequestration. *Am. J. Pathol.* **1985**, *119*, 385–401. [PubMed] [PubMed Central]

20. Hempel, C.; Combes, V.; Hunt, N.H.; Kurtzhals, J.A.; Grau, G.E. CNS hypoxia is more pronounced in murine cerebral than noncerebral malaria and is reversed by erythropoietin. *Am. J. Pathol.* **2011**, *179*, 1939–1950. [CrossRef] [PubMed] [PubMed Central]

21. Beare, N.A.; Harding, S.P.; Taylor, T.E.; Lewallen, S.; Molyneux, M.E. Perfusion abnormalities in children with cerebral malaria and malarial retinopathy. *J. Infect. Dis.* **2009**, *199*, 263–271. [CrossRef] [PubMed] [PubMed Central]

22. Medana, I.M.; Turner, G.D. Human cerebral malaria and the blood-brain barrier. *Int. J. Parasitol.* **2006**, *36*, 555–568. [CrossRef] [PubMed]

23. Greiner, J.; Dorovini-Zis, K.; Taylor, T.E.; Molyneux, M.E.; Beare, N.A.; Kamiza, S.; White, V.A. Correlation of hemorrhage, axonal damage, and blood-tissue barrier disruption in brain and retina of Malawian children with fatal cerebral malaria. *Front. Cell. Infect. Microbiol.* **2015**, *5*, 18. [CrossRef] [PubMed] [PubMed Central]

24. Penet, M.F.; Viola, A.; Confort-Gouny, S.; Le Fur, Y.; Duhamel, G.; Kober, F.; Ibarrola, D.; Izquierdo, M.; Coltel, N.; Gharib, B.; et al. Imaging experimental cerebral malaria in vivo: Significant role of ischemic brain edema. *J. Neurosci.* **2005**, *25*, 7352–7358. [CrossRef] [PubMed] [PubMed Central]

25. Seydel, K.B.; Kampondeni, S.D.; Valim, C.; Potchen, M.J.; Milner, D.A.; Muwalo, F.W.; Birbeck, G.L.; Bradley, W.G.; Fox, L.L.; Glover, S.J.; et al. Brain swelling and death in children with cerebral malaria. *N. Engl. J. Med.* **2015**, *372*, 1126–1137. [CrossRef] [PubMed] [PubMed Central]

26. Sahu, P.K.; Hoffmann, A.; Majhi, M.; Pattnaik, R.; Patterson, C.; Mahanta, K.C.; Mohanty, A.K.; Mohanty, R.R.; Joshi, S.; Mohanty, A.; et al. Brain Magnetic Resonance Imaging Reveals Different Courses of Disease in Pediatric and Adult Cerebral Malaria. *Clin. Infect. Dis.* **2021**, *73*, e2387–e2396. [CrossRef] [PubMed] [PubMed Central]

27. Hunt, N.H.; Grau, G.E. Cytokines: Accelerators and brakes in the pathogenesis of cerebral malaria. *Trends Immunol.* **2003**, *24*, 491–499. [CrossRef] [PubMed]

28. Conroy, A.L.; Lafferty, E.I.; Lovegrove, F.E.; Krudsood, S.; Tangpukdee, N.; Liles, W.C.; Kain, K.C. Whole blood angiopoietin-1 and -2 levels discriminate cerebral and severe (non-cerebral) malaria from uncomplicated malaria. *Malar. J.* **2009**, *8*, 295. [CrossRef] [PubMed] [PubMed Central]

29. Conroy, A.L.; Hawkes, M.; McDonald, C.R.; Kim, H.; Higgins, S.J.; Barker, K.R.; Namasopo, S.; Opoka, R.O.; John, C.C.; Liles, W.C.; et al. Host Biomarkers Are Associated With Response to Therapy and Long-Term Mortality in Pediatric Severe Malaria. *Open Forum Infect. Dis.* **2016**, *3*, ofw134. [CrossRef] [PubMed] [PubMed Central]

30. Lucchi, N.W.; Jain, V.; Wilson, N.O.; Singh, N.; Udhayakumar, V.; Stiles, J.K. Potential serological biomarkers of cerebral malaria. *Dis. Markers* **2011**, *31*, 327–335. [CrossRef] [PubMed] [PubMed Central]

31. Jain, V.; Lucchi, N.W.; Wilson, N.O.; Blackstock, A.J.; Nagpal, A.C.; Joel, P.K.; Singh, M.P.; Udhayakumar, V.; Stiles, J.K.; Singh, N. Plasma levels of angiopoietin-1 and -2 predict cerebral malaria outcome in Central India. *Malar. J.* **2011**, *10*, 383. [CrossRef] [PubMed] [PubMed Central]

32. Stins, M.F.; Mtaja, A.; Mulendele, E.; Mwimbe, D.W.; Pinilla, G.; Mutengo, M.; Pardo, C.A.; Chipeta, J. Elevated brain derived neurotrophic factor in plasma and interleukin-6 levels in cerebrospinal fluid in meningitis compared to cerebral malaria. *J. Neurol. Sci.* **2023**, *450*, 120663. [CrossRef] [PubMed] [PubMed Central]

33. Stins, M.F.; Mtaja, A.; Mulendele, E.; Mwimbe, D.; Pinilla-Monsalve, G.D.; Mutengo, M.; Pardo, C.A.; Chipeta, J. Inflammation and Elevated Osteopontin in Plasma and CSF in Cerebral Malaria Compared to Plasmodium-Negative Neurological Infections. *Int. J. Mol. Sci.* **2024**, *25*, 9620. [CrossRef] [PubMed] [PubMed Central]

34. Hunt, N.H.; Grau, G.E.; Engwerda, C.; Barnum, S.R.; van der Heyde, H.; Hansen, D.S.; Schofield, L.; Golenser, J. Murine cerebral malaria: The whole story. *Trends Parasitol.* **2010**, *26*, 272–274. [CrossRef] [PubMed]

35. Sahu, P.K.; Duffy, F.J.; Dankwa, S.; Vishnyakova, M.; Majhi, M.; Pirpamer, L.; Vigdorovich, V.; Bage, J.; Maharana, S.; Mandala, W.; et al. Determinants of brain swelling in pediatric and adult cerebral malaria. *JCI Insight* **2021**, *6*, e145823. [CrossRef] [PubMed] [PubMed Central]

36. Zhu, Y.; Gao, H.; Tong, L.; Li, Z.; Wang, L.; Zhang, C.; Yang, Q.; Yan, B. Emotion Regulation of Hippocampus Using Real-Time fMRI Neurofeedback in Healthy Human. *Front. Hum. Neurosci.* **2019**, *13*, 242. [CrossRef] [PubMed] [PubMed Central]

37. Bartsch, T.; Döhring, J.; Rohr, A.; Jansen, O.; Deuschl, G. CA1 neurons in the human hippocampus are critical for autobiographical memory, mental time travel, and autonoetic consciousness. *Proc. Natl. Acad. Sci. USA* **2011**, *108*, 17562–17567. [CrossRef] [PubMed] [PubMed Central]

38. Llorens-Martin, M.; Rabano, A.; Avila, J. The Ever-Changing Morphology of Hippocampal Granule Neurons in Physiology and Pathology. *Front. Neurosci.* **2015**, *9*, 526. [CrossRef] [PubMed] [PubMed Central]

39. Cho, K.O.; Lybrand, Z.R.; Ito, N.; Brulet, R.; Tafacory, F.; Zhang, L.; Good, L.; Ure, K.; Kernie, S.G.; Birnbaum, S.G.; et al. Aberrant hippocampal neurogenesis contributes to epilepsy and associated cognitive decline. *Nat. Commun.* **2015**, *6*, 6606. [CrossRef] [PubMed] [PubMed Central]

40. Belarbi, K.; Arellano, C.; Ferguson, R.; Jopson, T.; Rosi, S. Chronic neuroinflammation impacts the recruitment of adult-born neurons into behaviorally relevant hippocampal networks. *Brain Behav. Immun.* **2012**, *26*, 18–23. [CrossRef] [PubMed] [PubMed Central]

41. Llorens-Martin, M.; Jurado-Arjona, J.; Fuster-Matanzo, A.; Hernandez, F.; Rabano, A.; Avila, J. Peripherally triggered and GSK-3beta-driven brain inflammation differentially skew adult hippocampal neurogenesis, behavioral pattern separation and microglial activation in response to ibuprofen. *Transl. Psychiatry* **2014**, *4*, e463. [CrossRef] [PubMed] [PubMed Central]

42. De Souza, J.B.; Riley, E.M. Cerebral malaria: The contribution of studies in animal models to our understanding of immunopathogenesis. *Microbes Infect.* **2002**, *4*, 291–300. [CrossRef] [PubMed]

43. Kumar, S.P.; Babu, P.P. NADPH Oxidase: A Possible Therapeutic Target for Cognitive Impairment in Experimental Cerebral Malaria. *Mol. Neurobiol.* **2022**, *59*, 800–820. [CrossRef] [PubMed]

44. Dai, M.; Reznik, S.E.; Spray, D.C.; Weiss, L.M.; Tanowitz, H.B.; Gulinello, M.; Desruisseaux, M.S. Persistent cognitive and motor deficits after successful antimalarial treatment in murine cerebral malaria. *Microbes Infect.* **2010**, *12*, 1198–1207. [CrossRef] [PubMed] [PubMed Central]

45. Akide Ndunge, O.B.; Shikani, H.J.; Dai, M.; Freeman, B.D.; Desruisseaux, M.S. Effects of anti-tau immunotherapy on reactive microgliosis, cerebral endotheliopathy, and cognitive function in an experimental model of cerebral malaria. *J. Neurochem.* **2023**, *167*, 441–460. [CrossRef] [PubMed Central]

46. Stoltenburg-Didinger, G.; Neifer, S.; Bienzle, U.; Eling, W.M.; Kremsner, P.G. Selective damage of hippocampal neurons in murine cerebral malaria prevented by pentoxifylline. *J. Neurol. Sci.* **1993**, *114*, 20–24. [CrossRef] [PubMed]

47. Strangward, P.; Haley, M.J.; Shaw, T.N.; Schwartz, J.M.; Greig, R.; Mironov, A.; de Souza, J.B.; Cruickshank, S.M.; Craig, A.G.; Milner, D.A., Jr.; et al. A quantitative brain map of experimental cerebral malaria pathology. *PLoS Pathog.* **2017**, *13*, e1006267. [CrossRef] [PubMed] [PubMed Central]

48. Langhorne, J.; Buffet, P.; Galinski, M.; Good, M.; Harty, J.; Leroy, D.; Mota, M.M.; Pasini, E.; Renia, L.; Riley, E.; et al. The relevance of non-human primate and rodent malaria models for humans. *Malar. J.* **2011**, *10*, 23. [CrossRef] [PubMed] [PubMed Central]

49. Barrera, V.; Haley, M.J.; Strangward, P.; Attree, E.; Kamiza, S.; Seydel, K.B.; Taylor, T.E.; Milner, D.A., Jr.; Craig, A.G.; Couper, K.N. Comparison of CD8(+) T Cell Accumulation in the Brain During Human and Murine Cerebral Malaria. *Front. Immunol.* **2019**, *10*, 1747. [CrossRef] [PubMed] [PubMed Central]

50. Yanez, D.M.; Batchelder, J.; van der Heyde, H.C.; Manning, D.D.; Weidanz, W.P. Gamma delta T-cell function in pathogenesis of cerebral malaria in mice infected with Plasmodium berghei ANKA. *Infect. Immun.* **1999**, *67*, 446–448. [CrossRef] [PubMed] [PubMed Central]

51. Gramaglia, I.; Velez, J.; Chang, Y.S.; Caparros-Wanderley, W.; Combes, V.; Grau, G.; Stins, M.F.; van der Heyde, H.C. Citrulline protects mice from experimental cerebral malaria by ameliorating hypoargininemia, urea cycle changes and vascular leak. *PLoS ONE* **2019**, *14*, e0213428. [CrossRef] [PubMed] [PubMed Central]

52. Gramaglia, I.; Sobolewski, P.; Meays, D.; Contreras, R.; Nolan, J.P.; Frangos, J.A.; Intaglietta, M.; van der Heyde, H.C. Low nitric oxide bioavailability contributes to the genesis of experimental cerebral malaria. *Nat. Med.* **2006**, *12*, 1417–1422. [CrossRef] [PubMed]

53. Gramaglia, I.; Velez, J.; Combes, V.; Grau, G.E.; Wree, M.; van der Heyde, H.C. Platelets activate a pathogenic response to blood-stage Plasmodium infection but not a protective immune response. *Blood* **2017**, *129*, 1669–1679. [CrossRef] [PubMed] [PubMed Central]

54. Lee, M.H.; Wang, T.; Jang, M.H.; Steiner, J.; Haughey, N.; Ming, G.L.; Song, H.; Nath, A.; Venkatesan, A. Rescue of adult hippocampal neurogenesis in a mouse model of HIV neurologic disease. *Neurobiol. Dis.* **2011**, *41*, 678–687. [CrossRef] [PubMed] [PubMed Central]

55. Griffin, D.E. CSF changes during acute meningoencephalitis in mice caused by encephalomyocarditis virus. *Ann. Neurol.* **1981**, *10*, 55–57. [CrossRef] [PubMed]

56. Schindelin, J.; Arganda-Carreras, I.; Frise, E.; Kaynig, V.; Longair, M.; Pietzsch, T.; Preibisch, S.; Rueden, C.; Saalfeld, S.; Schmid, B.; et al. Fiji: An open-source platform for biological-image analysis. *Nat. Methods* **2012**, *9*, 676–682. [CrossRef] [PubMed] [PubMed Central]

57. Weidanz, W.P.; LaFleur, G.; Brown, A.; Burns, J.M., Jr.; Gramaglia, I.; van der Heyde, H.C. Gammadelta T cells but not NK cells are essential for cell-mediated immunity against Plasmodium chabaudi malaria. *Infect. Immun.* **2010**, *78*, 4331–4340. [CrossRef] [PubMed] [PubMed Central]

58. Medana, I.M.; Day, N.P.; Hien, T.T.; Mai, N.T.; Bethell, D.; Phu, N.H.; Farrar, J.; Esiri, M.M.; White, N.J.; Turner, G.D. Axonal injury in cerebral malaria. *Am. J. Pathol.* **2002**, *160*, 655–666. [CrossRef] [PubMed] [PubMed Central]

59. Barro, C.; Zetterberg, H. Neurological symptoms and blood neurofilament light levels. *Acta Neurol. Scand.* **2021**, *144*, 13–20. [CrossRef] [PubMed]

60. Wai, C.H.; Jin, J.; Cyrklaff, M.; Genoud, C.; Funaya, C.; Sattler, J.; Maceski, A.; Meier, S.; Heiland, S.; Lanzer, M.; et al. Neurofilament light chain plasma levels are associated with area of brain damage in experimental cerebral malaria. *Sci. Rep.* **2022**, *12*, 10726. [CrossRef] [PubMed] [PubMed Central]

61. Balanza, N.; Francis, C.K.; Crowley, V.M.; Weckman, A.M.; Zhong, K.; Baro, B.; Varo, R.; Bassat, Q.; Kain, K.C. Reply to Zayet et al. *J. Infect. Dis.* **2024**, *229*, 296–297. [CrossRef] [PubMed]

62. Datta, D.; Gopinadhan, A.; Soto, A.; Bangirana, P.; Opoka, R.O.; Conroy, A.L.; Saykin, A.J.; Kawata, K.; John, C.C. Blood biomarkers of neuronal injury in paediatric cerebral malaria and severe malarial anaemia. *Brain Commun.* **2023**, *5*, fcad323. [CrossRef] [PubMed] [PubMed Central]

63. Datta, D.; Conroy, A.L.; Castelluccio, P.F.; Ssenkusu, J.M.; Park, G.S.; Opoka, R.O.; Bangirana, P.; Idro, R.; Saykin, A.J.; John, C.C. Elevated Cerebrospinal Fluid Tau Protein Concentrations on Admission Are Associated With Long-term Neurologic and Cognitive Impairment in Ugandan Children With Cerebral Malaria. *Clin. Infect. Dis.* **2020**, *70*, 1161–1168. [CrossRef] [PubMed] [PubMed Central]

64. Leitner, D.F.; Stoute, J.A.; Landmesser, M.; Neely, E.; Connor, J.R. The HFE genotype and a formulated diet controlling for iron status attenuate experimental cerebral malaria in mice. *Int. J. Parasitol.* **2015**, *45*, 797–808. [CrossRef] [PubMed]

65. Hempel, C.; Hyttel, P.; Staalsø, T.; Nyengaard, J.R.; Kurtzhals, J.A. Erythropoietin treatment alleviates ultrastructural myelin changes induced by murine cerebral malaria. *Malar. J.* **2012**, *11*, 216. [CrossRef] [PubMed] [PubMed Central]

66. Noël, A.; Zhou, L.; Foveau, B.; Sjöström, P.J.; LeBlanc, A.C. Differential susceptibility of striatal, hippocampal and cortical neurons to Caspase-6. *Cell Death Differ.* **2018**, *25*, 1319–1335. [CrossRef] [PubMed] [PubMed Central]

67. Medana, I.M.; Day, N.P.; Hien, T.T.; Mai, N.T.; Bethell, D.; Phu, N.H.; Turner, G.D.; Farrar, J.; White, N.J.; Esiri, M.M. Cerebral calpain in fatal falciparum malaria. *Neuropathol. Appl. Neurobiol.* **2007**, *33*, 179–192. [CrossRef] [PubMed]

68. Villabona-Rueda, A.; Erice, C.; Pardo, C.A.; Stins, M.F. The Evolving Concept of the Blood Brain Barrier (BBB): From a Single Static Barrier to a Heterogeneous and Dynamic Relay Center. *Front. Cell. Neurosci.* **2019**, *13*, 405. [CrossRef] [PubMed] [PubMed Central]

69. Szklarczyk, A.; Stins, M.; Milward, E.A.; Ryu, H.; Fitzsimmons, C.; Sullivan, D.; Conant, K. Glial activation and matrix metalloproteinase release in cerebral malaria. *J. Neurovirol.* **2007**, *13*, 2–10. [CrossRef] [PubMed]

70. Hochman, S.E.; Madaline, T.F.; Wassmer, S.C.; Mbale, E.; Choi, N.; Seydel, K.B.; Whitten, R.O.; Varughese, J.; Grau, G.E.; Kamiza, S.; et al. Fatal Pediatric Cerebral Malaria Is Associated with Intravascular Monocytes and Platelets That Are Increased with HIV Coinfection. *MBio* **2015**, *6*, e01390-15. [CrossRef]

71. Medana, I.M.; Idro, R.; Newton, C.R. Axonal and astrocyte injury markers in the cerebrospinal fluid of Kenyan children with severe malaria. *J. Neurol. Sci.* **2007**, *258*, 93–98. [CrossRef] [PubMed]

72. Mandala, W.L.; Msefula, C.L.; Gondwe, E.N.; Drayson, M.T.; Molyneux, M.E.; MacLennan, C.A. Cytokine Profiles in Malawian Children Presenting with Uncomplicated Malaria, Severe Malarial Anemia, and Cerebral Malaria. *Clin. Vaccine Immunol.* **2017**, *24*, e00533-16. [CrossRef] [PubMed] [PubMed Central]

73. Tran, H.; Gupta, M.; Gupta, K. Targeting novel mechanisms of pain in sickle cell disease. *Blood* **2017**, *130*, 2377–2385. [CrossRef] [PubMed] [PubMed Central]

74. Wassmer, S.C.; Moxon, C.A.; Taylor, T.; Grau, G.E.; Molyneux, M.E.; Craig, A.G. Vascular endothelial cells cultured from patients with cerebral or uncomplicated malaria exhibit differential reactivity to TNF. *Cell. Microbiol.* **2011**, *13*, 198–209. [CrossRef] [PubMed] [PubMed Central]

75. Bonaguidi, M.A.; Stadel, R.P.; Berg, D.A.; Sun, J.; Ming, G.L.; Song, H. Diversity of Neural Precursors in the Adult Mammalian Brain. *Cold Spring Harb. Perspect. Biol.* **2016**, *8*, a018838. [CrossRef] [PubMed] [PubMed Central]

76. Satish Bollimpelli, V.; Kondapi, A.K. Differential sensitivity of immature and mature ventral mesencephalic neurons to rotenone induced neurotoxicity in vitro. *Toxicol. Vitr.* **2015**, *30*, 545–551. [CrossRef] [PubMed]

77. Klein, B.; Mrowetz, H.; Kreutzer, C.; Rotheneichner, P.; Zaunmair, P.; Lange, S.; Coras, R.; Couillard-Despres, S.; Rivera, F.J.; Aigner, L. DCX(+) neuronal progenitors contribute to new oligodendrocytes during remyelination in the hippocampus. *Sci. Rep.* **2020**, *10*, 20095. [CrossRef] [PubMed] [PubMed Central]

78. Bennett, L.; Yang, M.; Enikolopov, G.; Iacovitti, L. Circumventricular organs: A novel site of neural stem cells in the adult brain. *Mol. Cell. Neurosci.* **2009**, *41*, 337–347. [CrossRef] [PubMed] [PubMed Central]

79. de Miranda, A.S.; Brant, F.; Campos, A.C.; Vieira, L.B.; Rocha, N.P.; Cisalpino, D.; Binda, N.S.; Rodrigues, D.H.; Ransohoff, R.M.; Machado, F.S.; et al. Evidence for the contribution of adult neurogenesis and hippocampal cell death in experimental cerebral malaria cognitive outcome. *Neuroscience* **2015**, *284*, 920–933. [CrossRef] [PubMed]

80. Tosun, M.; Semerci, F.; Maletic-Savatic, M. Heterogeneity of Stem Cells in the Hippocampus. *Adv. Exp. Med. Biol.* **2019**, *1169*, 31–53. [CrossRef] [PubMed]

81. Ruiz-Clavijo, L.; Martín-Suárez, S. The differential response to neuronal hyperexcitation and neuroinflammation of the hippocampal neurogenic niche. *Front. Neurosci.* **2023**, *17*, 1186256. [CrossRef] [PubMed] [PubMed Central]

82. Clark, D.J.; Bond, C.; Andrews, A.; Muller, D.J.; Sarkisian, A.; Opoka, R.O.; Idro, R.; Bangirana, P.; Witten, A.; Sausen, N.J.; et al. Admission Clinical and EEG Features Associated With Mortality and Long-term Neurologic and Cognitive Outcomes in Pediatric Cerebral Malaria. *Neurology* **2023**, *101*, e1307–e1318. [CrossRef] [PubMed] [PubMed Central]

83. Bangirana, P.; Opoka, R.O.; Boivin, M.J.; Idro, R.; Hodges, J.S.; John, C.C. Neurocognitive domains affected by cerebral malaria and severe malarial anemia in children. *Learn. Individ. Differ.* **2016**, *46*, 38–44. [CrossRef] [PubMed] [PubMed Central]